NASA/TM-1999-208970

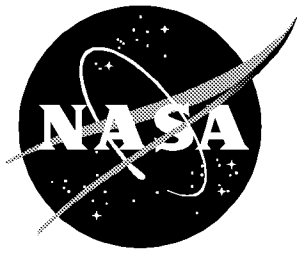

Demonstration of Imaging Flow Diagnostics Using Rayleigh Scattering in Langley 0.3-Meter Transonic Cryogenic Tunnel

B. Shirinzadeh and G. C. Herring
Langley Research Center, Hampton, Virginia

Toya Barros
Spelman College, Atlanta, Georgia

February 1999

The NASA STI Program Office . . . in Profile

Since its founding, NASA has been dedicated to the advancement of aeronautics and space science. The NASA Scientific and Technical Information (STI) Program Office plays a key part in helping NASA maintain this important role.

The NASA STI Program Office is operated by Langley Research Center, the lead center for NASA's scientific and technical information. The NASA STI Program Office provides access to the NASA STI Database, the largest collection of aeronautical and space science STI in the world. The Program Office is also NASA's institutional mechanism for disseminating the results of its research and development activities. These results are published by NASA in the NASA STI Report Series, which includes the following report types:

- TECHNICAL PUBLICATION. Reports of completed research or a major significant phase of research that present the results of NASA programs and include extensive data or theoretical analysis. Includes compilations of significant scientific and technical data and information deemed to be of continuing reference value. NASA counterpart or peer-reviewed formal professional papers, but having less stringent limitations on manuscript length and extent of graphic presentations.

- TECHNICAL MEMORANDUM. Scientific and technical findings that are preliminary or of specialized interest, e.g., quick release reports, working papers, and bibliographies that contain minimal annotation. Does not contain extensive analysis.

- CONTRACTOR REPORT. Scientific and technical findings by NASA-sponsored contractors and grantees.

- CONFERENCE PUBLICATION. Collected papers from scientific and technical conferences, symposia, seminars, or other meetings sponsored or co-sponsored by NASA.

- SPECIAL PUBLICATION. Scientific, technical, or historical information from NASA programs, projects, and missions, often concerned with subjects having substantial public interest.

- TECHNICAL TRANSLATION. English-language translations of foreign scientific and technical material pertinent to NASA's mission.

Specialized services that complement the STI Program Office's diverse offerings include creating custom thesauri, building customized databases, organizing and publishing research results . . . even providing videos.

For more information about the NASA STI Program Office, see the following:

- Access the NASA STI Program Home Page at *http://www.sti.nasa.gov*

- Email your question via the Internet to help@sti.nasa.gov

- Fax your question to the NASA STI Help Desk at (301) 621-0134

- Telephone the NASA STI Help Desk at (301) 621-0390

- Write to:
  NASA STI Help Desk
  NASA Center for AeroSpace Information
  7121 Standard Drive
  Hanover, MD 21076-1320

NASA/TM-1999-208970

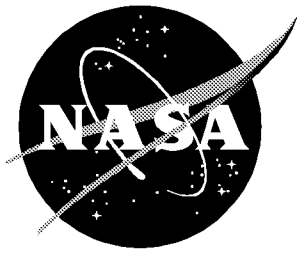

Demonstration of Imaging Flow Diagnostics Using Rayleigh Scattering in Langley 0.3-Meter Transonic Cryogenic Tunnel

B. Shirinzadeh and G. C. Herring
Langley Research Center, Hampton, Virginia

Toya Barros
Spelman College, Atlanta, Georgia

National Aeronautics and
Space Administration

Langley Research Center
Hampton, Virginia 23681-2199

February 1999

Acknowledgments

W. E. Lipford, Langley Research Center, helped with the wind tunnel installation of the Rayleigh setup. J. B. Anders, Langley Research Center, and R. Valla, McDonnell Douglas Corporation, let us piggyback on their tunnel time. We thank the staff of the Langley 0.3-Meter Transonic Cryogenic Tunnel (especially M. Chambers) for their support during this work.

Available from:

NASA Center for AeroSpace Information (CASI)
7121 Standard Drive
Hanover, MD 21076-1320
(301) 621-0390

National Technical Information Service (NTIS)
5285 Port Royal Road
Springfield, VA 22161-2171
(703) 605-6000

Abstract

The feasibility of using the Rayleigh scattering technique for molecular density imaging of the free-stream flow field in the Langley 0.3-Meter Transonic Cryogenic Tunnel has been experimentally demonstrated. The Rayleigh scattering was viewed with a near-backward geometry with a frequency-doubled output from a diode-pumped CW Nd:YAG laser and an intensified charge-coupled device camera. Measurements performed in the range of free-stream densities from 3×10^{25} *to* 24×10^{25} *molecules/m*^{3} *indicate that the observed relative Rayleigh signal levels are approximately linear with flow field density. The absolute signal levels agree (within ≈30 percent) with the expected signal levels computed based on the well-known quantities of flow field density, Rayleigh scattering cross section for* N_2*, solid angle of collection, transmission of the optics, and the independently calibrated camera sensitivity. These results show that the flow field in this facility is primarily molecular (i.e., not contaminated by clusters) and that Rayleigh scattering is a viable technique for quantitative nonintrusive diagnostics in this facility.*

Introduction

The application of nonintrusive optical techniques to wind tunnel diagnostics has been an active area of aeronautics research for 30 years. With the invention of high-power lasers and multipoint detectors like charge-coupled device (CCD) cameras, line or planar measurements of flow quantities such as density, temperature, and velocity have opened new areas in fluid mechanics research. Flow density visualization using Rayleigh scattering (ref. 1), one of many laser techniques, is the subject of this report.

Over the last decade, our group in the Measurement Science and Technology Branch has undertaken an effort to apply Rayleigh scattering to various wind tunnels at the Langley Research Center (LaRC). This program has resulted in, among other results, qualitative studies of fuel-air mixing (ref. 2) and quantitative measurements of the density profiles of strong shocks (ref. 3), both at Mach 6. We have learned that typical run conditions in the free stream of many supersonic dry-air wind tunnels are conducive to clustering. Although sometimes useful for qualitative flow visualization, clustering prohibits the use of Rayleigh scattering for quantitative density studies because under these conditions the signal behaves highly nonlinear with the flow density. This nonlinearity is caused by the rapid increase of the Rayleigh scattering signal (cross section) with the size of the clusters.

We are interested in extending our work to subsonic and transonic tunnels that are of interest to the commercial aeronautics sector. Some subsonic tunnels work at cryogenic temperatures (≈100 K) to increase the Reynolds numbers to approach atmospheric flight conditions. An example is the Langley 0.3-Meter Transonic Cryogenic Tunnel (0.3-mTCT), which uses N_2 instead of air. In planning Rayleigh diagnostics for cryogenic tunnels, one of the early questions to answer is, "Does clustering occur at typical run conditions?" Clustering in air usually occurs easier than in pure N_2 because of the presence of Ar, O_2, and CO_2. However, in facilities that use pure N_2, clustering is still a concern (ref. 4). The purpose of this work is to determine whether clustering occurs in the 0.3-mTCT and to demonstrate the feasibility of quantitative density measurements using Rayleigh scattering.

Rayleigh Scattering

A well-rounded summary of Rayleigh scattering is given in reference 5. For the Rayleigh scattered light that is imaged onto a single photodetector, the magnitude of the signal collected at 90° relative to the polarization of the beam is given by

$$P = N\left(\frac{d\sigma}{d\Omega}\right)_{90} LP_1 \varepsilon \eta \Omega \tag{1}$$

where P is the scattered light signal (photoelectrons per second) that is detected, Ω is the solid angle (steradians) used to collect that scattered light, η is the total transmission of the collection optics from the sample volume to the detector cathode, P_1 (photons per second) is the incident power of the laser beam in the sample volume, ε is the quantum efficiency of the detector cathode, and L (meters) is the length of the laser beam that is imaged onto the detector. The differential scattering cross section per molecule (meter^2 per (steradian-molecule)) at 90° to the polarization direction is denoted by $(d\sigma/d\Omega)_{90}$. Finally, N is the number density (molecules per meter^3) of the scattering medium. Equation (1) is written as if all the scattered light that is collected in the solid angle Ω is directed onto one detector cathode (i.e., a nonimaging mode).

If one is imaging the extended sample volume onto a camera, equation (1) must be used slightly differently. In our case, we are analyzing the signal on only one row (e.g., the center of the laser beam) of camera pixels (parallel to the beam propagation direction). The fraction of total laser power that corresponds to that row of pixels is used for P_1 in equation (1); thus, one must know the size and shape of the laser beam in the sample volume.

If not observing the sample volume at 90° to both the beam direction and polarization, two other potential corrections to equation (1) need to be made. The 90° cross section may still be used as long as the observation is in the plane perpendicular to the electric field polarization and parallel to the beam propagation direction. The cross section is not a function of observation direction in this special plane. The cross section must be corrected when observing from outside this plane. For our geometry, because we are observing from this special plane, we can use the 90° cross section. Second, equation (1) is appropriate for these observations only if one corrects the sample length L (i.e., increases L from its 90° value) for the geometrical effect of not observing the sample volume at 90° to the beam direction.

Experimental Apparatus

This work was performed in the 0.3-mTCT, which is a fan-driven, closed-circuit facility (ref. 6) designed to achieve large Reynolds numbers ($\approx 3 \times 10^8$/m) by using high-pressure (≈5 atm) and low-temperature (≈100 K) N_2 as the flow medium. This two-dimensional (2-D) tunnel is used primarily for the testing of 2-D airfoil configurations and for testing potential technology for its larger sister facility, the National Transonic Facility (NTF).

A schematic of the Rayleigh apparatus as it was used in the 0.3-mTCT is shown in figure 1. This view is cross sectional, with the flow coming towards the reader (out of the plane of the paper). An 80-mW CW Nd:YAG laser is weakly focused on the centerline of the test section with lenses L1 and L2. The laser is linearly polarized, with the polarization rotated with the 1/2-λ waveplate to be parallel to the free-stream flow direction (i.e., out of the plane of the paper in fig. 1). About one half, 40 mW, of the power is transmitted to the test section region.

An approximately 5-cm-long region centered on the centerline of the test section is imaged (reduced by a factor of 1/5 magnification) onto the photocathode of the intensified charge-coupled

device (ICCD) camera with the combination of lenses L3, L4, L5, and L6. In this way, a line image of the Rayleigh signal along a few rows of pixels (Pixel dimension = 30 μm wide by 18 μm high) is obtained. The observation direction is about 25° from the laser beam in a near-backward scattering geometry. The ICCD camera is operated at the standard video rate of 1/60 sec/field, with 2 fields per full frame. In addition, the scatter in the quasi-forward direction was also imaged with a nonintensified video rate camera at an angle of about 25° relative to the beam direction. The sensitivity of this camera is not sufficient to detect the molecular Rayleigh signals but is sufficient to detect the scattering of the laser beam from the windows or large clusters, if present.

Results and Discussion

Rayleigh Scattering

The images from both cameras were recorded directly on videotape at the standard video rate of 1/30 sec during the tunnel runs and later digitized with a commercially available digitizer. Figure 2(a) shows the beam image from the first field of a single frame, whereas figure 2(b) shows the average of 92 successive images (first field only) acquired over 3 sec. We have omitted the second field from the data shown in figure 2. The free-stream test section conditions are static pressure of 0.43 MN/m^2, static temperature of 255 K, and Mach 0.6.

Figure 3 shows the light level for a single vertical column of pixels, through the brightest portion of the beam for a 92 image average such as that shown in figure 2. The narrow bright portion at about pixel 107 of the laser beam can easily be distinguished from the background of scatter from various sources (primarily the windows). The net Rayleigh signal is estimated by subtracting the background. The net Rayleigh signal, in this case, is 28 – 15 = 13 counts. The background level at pixel numbers less that 45 has been deleted because this region is dominated by the time code information (fig. 2) that is written at the top of each frame. The data shown in figure 3 show a typical signal-to-background ratio. For some run conditions, the signal-to-background ratio is significantly worse than that shown in figure 3 because of increased background level. Thus, we have averaged many data points and tunnel runs to determine the Rayleigh scattered light dependence on the free-stream density.

Figure 4 shows 44 data points for a variety of tunnel pressures and temperatures. The pressure and temperature combinations are always set to provide one of six different free-stream densities. Because we piggybacked on another primary tunnel test, these six densities were chosen for the purposes of the other test. Each datum point is an average of 92 images (i.e., 3-sec integration) such as that shown in figure 3. Less than 44 data points are distinguishable because some data points exactly overlap.

The large scatter in the data of figure 4 is primarily due to four reasons. Statistical noise is significant because the signal-to-noise level is small for a good fraction of our data. Three other factors contribute systematic errors. First, the small signal-to-background level can contribute error if we do not estimate the background accurately. Second, we did not initially plan for a continuous power monitor because the laser was stable in the laboratory preparation work. However, the laser power varied much more in the severe temperature changes of the test cell. In addition, these power fluctuations are accompanied by gross changes in the spatial mode. Because we are analyzing only a fraction of the Rayleigh signal produced by a fraction of the laser profile, these mode fluctuations minimize the effectiveness of normalizing by the total power. Lack of access to the test cell during the tunnel runs allowed only a few scattered laser power measurements between data points. Thus, the laser power was not measured for each data point. Laser power fluctuations that were typically 20 percent, or 50 percent at most, contribute significantly to the spread in the data of figure 4 . Third, because some of the signals are close to the detection limit of the camera, they are affected by digitization noise.

The procedure used in generating figure 4 was repeated twice to accumulate three times the data shown. The two additional data sets agree with the one shown in figure 4. The results of these approximately 130 data points are averaged for each of the six densities and shown in figure 5. The uncertainties shown are the ±95 percent confidence levels for the means (not the populations). The number of data points averaged at each density is different because the fraction of time at a given density was determined by the primary tunnel test occurring simultaneously with our test. The number of points averaged from low to high density is 3, 12, 27, 6, 39, and 44. To within the statistical uncertainty of ±95 percent confidence, we conclude that the observed light scatter signal is roughly linear with density.

The straight line shown in figure 5 is a calculation, with equation (1), of the expected Rayleigh signal from molecular N_2 for these densities. The uncertainty in this calculation is dominated by the uncertainty in the laser power, about a factor of 2. In addition, the uncertainty is slightly increased because the collection solid angle and the detector sensitivity are both known to about 10 to 20 percent. Thus, the total uncertainty in our calculation is about a factor of 2 to 3. The relatively good agreement (i.e., less than a factor of 2) between experiment and calculation convinces us that the signals that were detected are due to Rayleigh scatter from molecules and not clusters. We would expect to observe a signal that is orders of magnitude greater than that predicted by equation (1) if clustering was occurring. The linearity of the signal with density reinforces the conclusion of negligible clustering under normal run conditions for this facility. This conclusion is in agreement with previous laser Doppler velocimetry (refs. 7 to 9), which did not find large particles in the natural and normal flow.

Observation of CO_2 Condensation

In this section, an interesting observation is discussed. We believe that we can detect the condensation of CO_2 on the plenum side of the inner windows. Before cooling to cryotemperatures, the facility is purged with N_2 at room temperature to remove room air. CO_2 exists in the N_2 supply as a small (5 ppm) impurity and in the residual air that is not completely purged from the plenum. This condensation is observed by measuring the brightness of the scatter of the laser beam where it propagates through the test section windows (i.e., the inner windows of fig. 1). The brightness of the scatter is taken from the signal levels from the unintensified CCD video camera. The temperature of the windows was determined by mounting a thermocouple on the outside wall of the test section, near one of the inside windows shown in figure 1.

With the CCD video camera that looks at the forward scatter with a wide field of view, we observe the scatter from the points where the beam intersects both the outside and inside surfaces of the test section windows. We can easily resolve the two (inside and outside) spots on the closer window. If the tunnel is run for long periods of time at 255 K, for example, we observe relatively weak scatter for the outside spot (the side of the window facing the plenum not the test section). This same scatter on the outside of the window steadily grows brighter with time after the test section has been cooled down below about 200 K. Below 200 K, this pronounced scatter from the windows is worse (brighter) with short purge times (5 min) and is better (dimmer) with long purge times (30 min).

The strongest evidence for our assertion of CO_2 condensation is observed when the tunnel is warmed back to room temperature. As the temperature of the test section passes the region near 225 K the scatter from the outside spot quickly gets much weaker. This happens over a period of 2 min, whereas the entire warm-up time from 150 K to room temperature is typically a few hours. Thus, the large reduction in scatter occurs within a few degrees of 225 K. At $\approx$0.1 MN/m^2 (i.e.,1 atm), CO_2 sublimates from a solid to a gas at about 225 K. Thus, we postulate that we are observing the condensation of CO_2 when cooling below 225 K and sublimation when warming above 225 K on the outside window

face that is in the plenum. We observed this behavior on all three different warm-up cycles that were monitored for this effect.

This temperature-dependent behavior was not seen on the inside face of the test section window. On the inside window face, the brightness of the beam scatter was observed to slowly increase with the total time that the tunnel had been run regardless of temperature. When the test section was open, we were able to clean both window faces, and clearly oil was on the inside faces but no sign of oil was on the outside face. Thus we are seeing two effects: temperature-independent oil accumulation on the inside faces of the test section windows, and strong temperature-dependent CO_2 condensation (and subsequent sublimation) on the outside faces of the test section windows.

Future work using optical diagnostics and windows will have to circumvent this condensation problem. Although the condensation seems to occur only on the plenum side of the windows, we suspect that the plenum does not get purged with N_2 as well as the test section because of restricted flow between the two cavities. Thus, the extremely smooth finishes on the model surfaces that are required for work at high Reynolds numbers are probably not being compromised by condensation of CO_2.

Concluding Remarks

The feasibility of Rayleigh scattering diagnostics on the high-density ($\approx 3 \times 10^{26}$ molecules/m^3) N_2, free-stream flow field in the Langley 0.3-Meter Transonic Cryogenic Tunnel (0.3-mTCT) has been experimentally demonstrated. With a near-backward scattering geometry, we have imaged a CW 40-mW laser beam at 532 nm using an intensified charge-coupled device (ICCD) camera. The observed relative Rayleigh signal levels are approximately linear with flow field density. The absolute signal levels also agree (within $\approx$30 percent) with expected signal levels based on the well-known quantities of flow field density, Rayleigh scattering cross section for N_2, and the camera sensitivity, which is independently calibrated. These results show that the flow field in the 0.3-mTCT is primarily molecular (i.e., not contaminated by clustering). Thus, Rayleigh scattering is a viable technique for quantitative nonintrusive diagnostics in the 0.3-mTCT and, possibly, its larger sister facility, the National Transonic Facility. In addition, this work shows that, in the 0.3-mTCT, imaging of the flow field density is possible.

References

1. Escoda, M. C.; and Long, M. B.: Rayleigh Scattering Measurements of the Gas Concentration Field in Turbulent Jets. *AIAA J.*, vol. 21, Jan. 1983, pp. 81–84.

2. Shirinzadeh, B.; Hillard, M. E.; Balla, R. Jeffrey; Waitz, I. A.; Anders, J. B.; and Exton, R. J.: Planar Rayleigh Scattering Results in Helium—Air Mixing Experiments in a Mach-6 Wind Tunnel. *Appl. Opt.*, vol. 31, no. 30, Oct. 1992, pp. 6529–6534.

3. Shirinzadeh, B.; Balla, R. Jeffrey; and Hillard, M. E.: Quantitative Density Measurements in a Mach 6 Flow Field Using the Rayleigh Scattering Technique. *ICIASF '95*, IEEE Publ. 95CH3482-7, July 1995, pp. 13.1–13.7.

4. Wegener, P. P.: Cryogenic Transonic Wind Tunnels and the Condensation of Nitrogen. *Exp. Fluids*, vol. 11, no. 5, Sept. 1991, pp. 333–338.

5. Eckbreth, A. C.: *Laser Diagnostics for Combustion Temperature and Species.* Abacus Press, 1988, pp. 209–214.

6. Balakrishna, S.; and Kilgore, W. Allen: *Performance of the 0.3-Meter Transonic Cryogenic Tunnel With Air, Nitrogen, and Sulfur Hexafluoride Media Under Closed Loop Automatic Control.* NASA CR-195052, 1995.

7. Gartrell, L. R.; Gooderum, P. B.; Hunter, W. W., Jr.; and Meyers, J. F.: *Laser Velocimetry Technique Applied to the Langley 0.3 Meter Transonic Cryogenic Tunnel.* NASA TM-81913, 1981, p. 8.

8. Honaker, W. C.; and Lawing, P. L.: *Measurements in the Flow Field of a Cylinder With a Laser Transit Anemometer and a Drag Rake in the Langley 0.3 m Transonic Cryogenic Tunnel.* NASA TM-86399, 1985, p. 5.

9. Selby, G. V.: *Vapor-Screen Flow-Visualization Experiments in the NASA Langley 0.3-m Transonic Cryogenic Tunnel.* NASA CR-3984, 1986, p. 6.

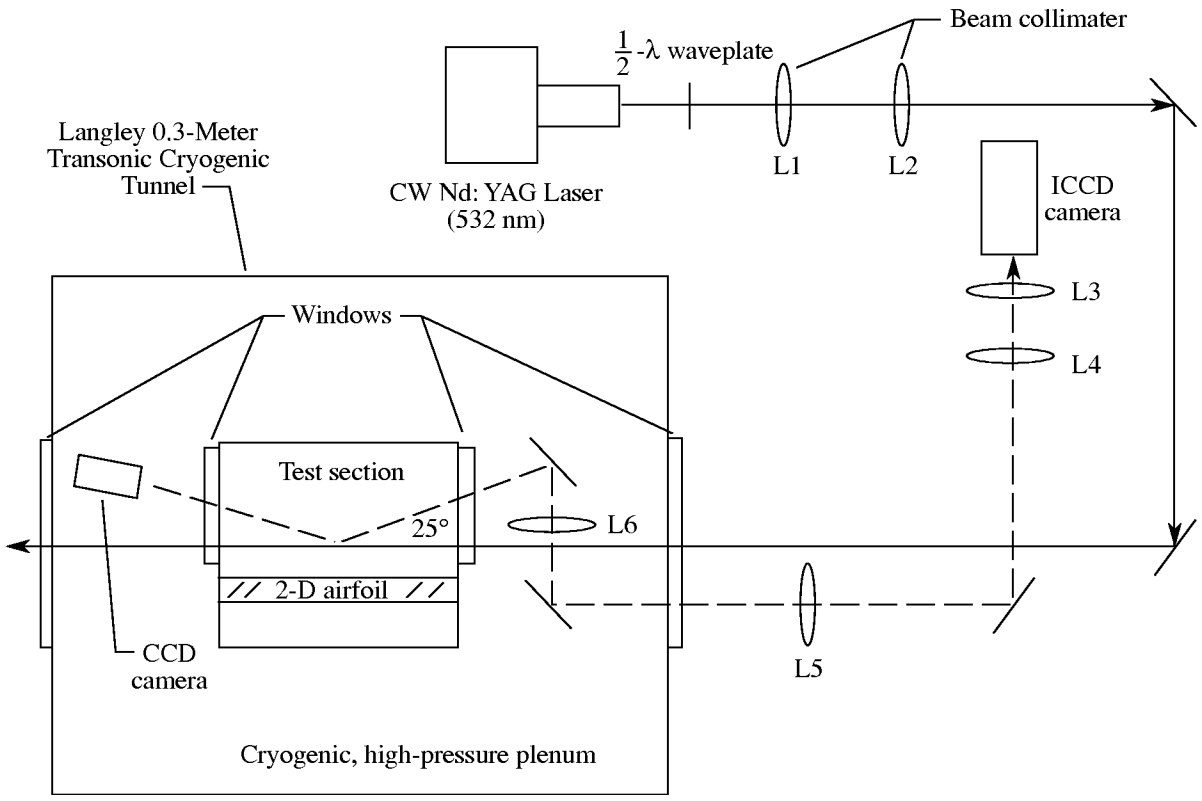

Figure 1. Schematic of experimental setup of Rayleigh instrument in test section of 0.3-mTCT.

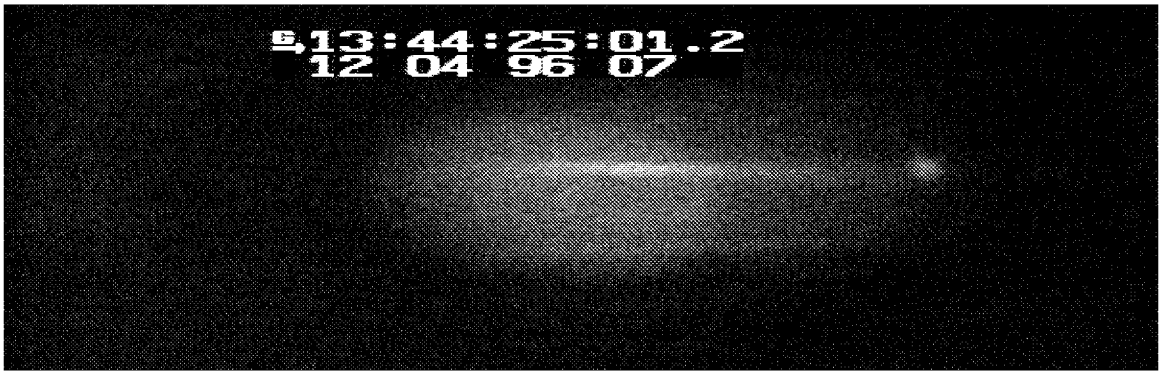

(a) Single field of one frame.

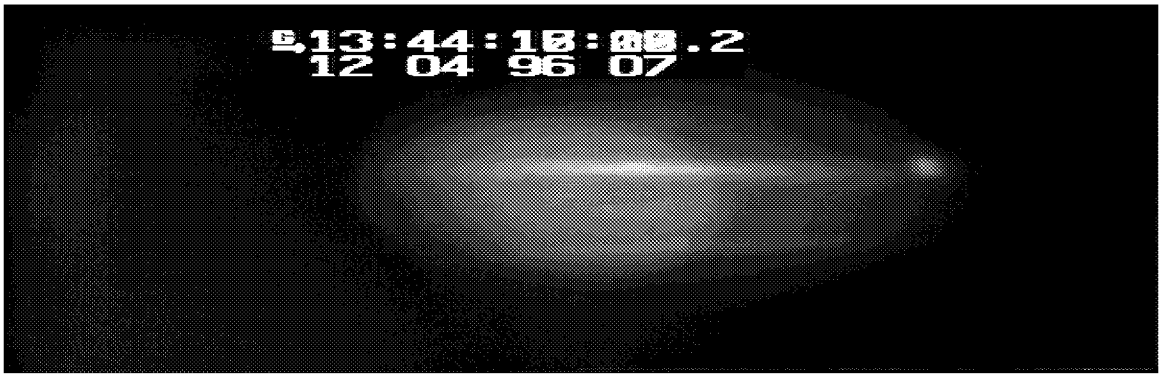

(b) Averaged over 92 frames.

Figure 2. Raw images of laser beam as it appears in quasi-backward direction. Free-stream flow conditions: Mach, 0.6; static pressure, 0.43 MN/m^2; static temperature, 255 K.

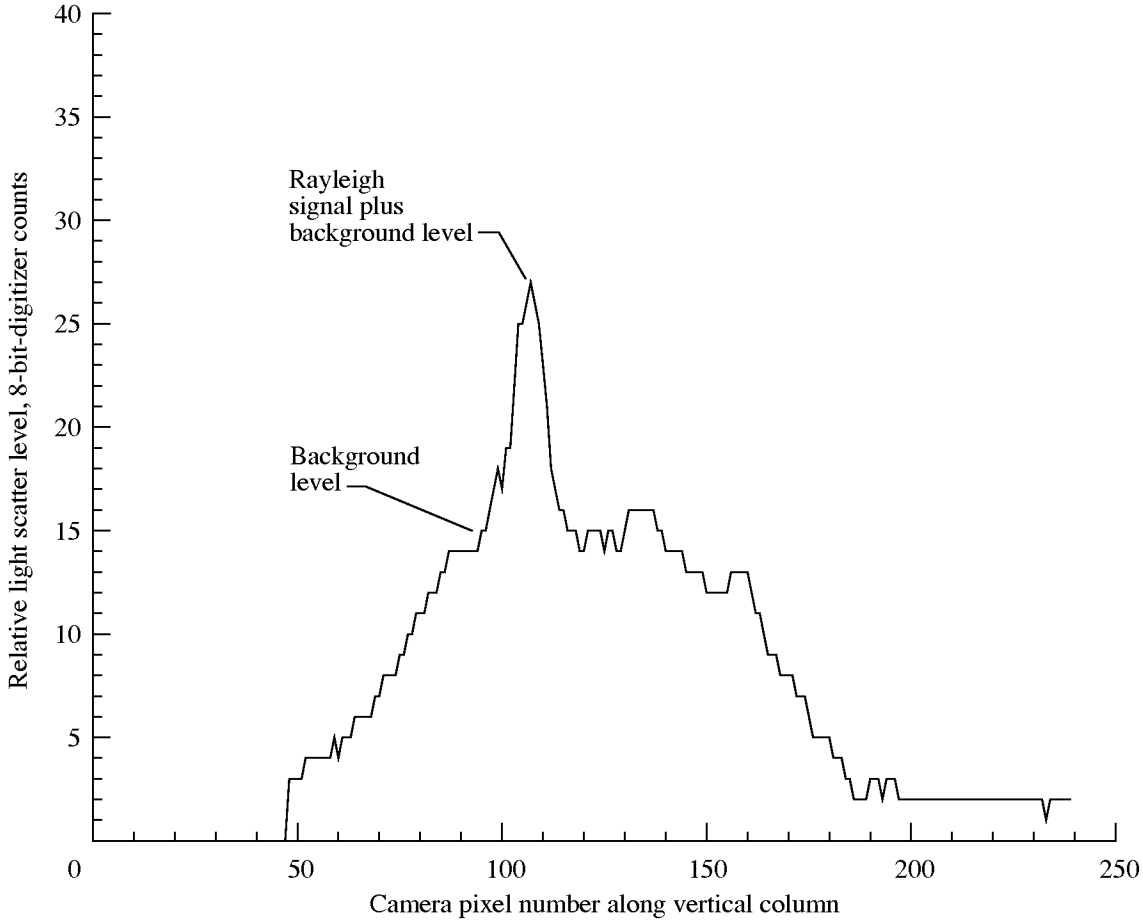

Figure 3. One column of pixels from 92-image average similar to that shown in figure 2. Free-stream fluid conditions: Mach, 0.6; static pressure, 0.43 MN/m^2; static temperature, 255 K.

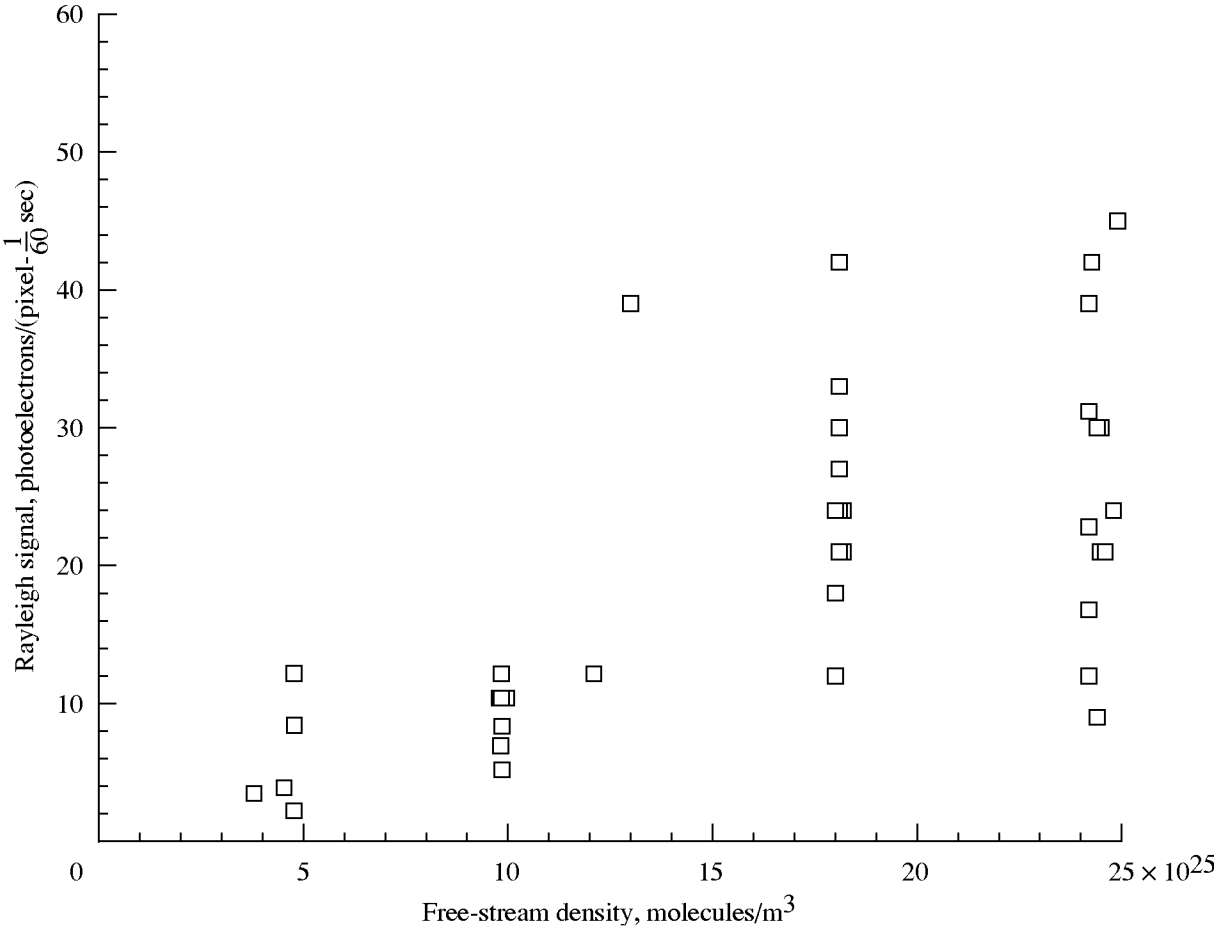

Figure 4. Summary of 44 data points (each point derived from 92-image average similar to that of figure 2(b)) for a variety of free-stream pressures, temperatures, and Mach numbers. Combinations of temperature and pressure are always selected to give one of six densities shown in figure; 44 points are not distinguishable because some points overlap.

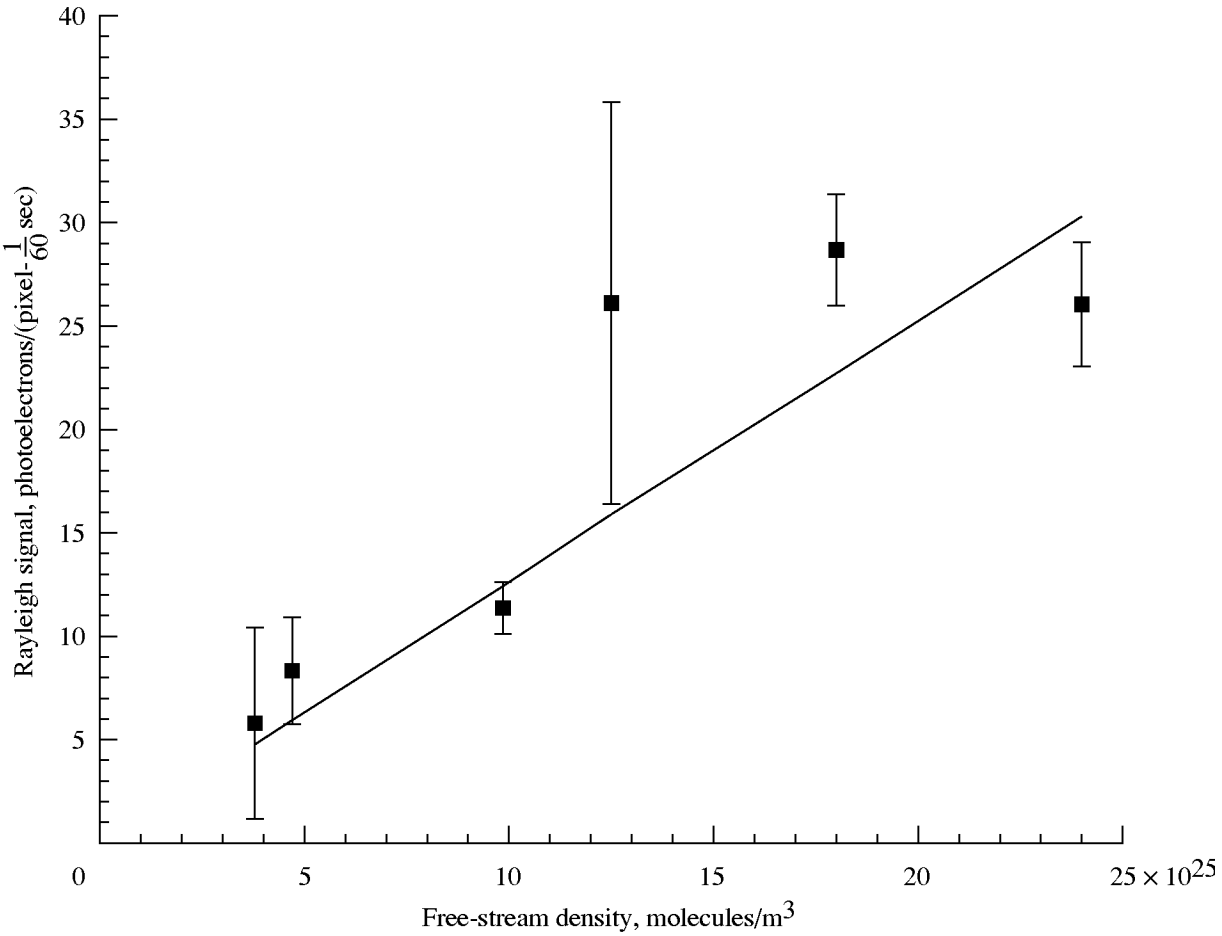

Figure 5. Average of about 130 data points, including 44 shown in figure 4. Displayed uncertainties are ±95 percent confidence limits based only on statistics (not systematic errors); solid line is expected Rayleigh signal from molecular N_2 calculated from equation (1).

REPORT DOCUMENTATION PAGE

Form Approved
OMB No. 07704-0188

1. AGENCY USE ONLY *(Leave blank)*	2. REPORT DATE	3. REPORT TYPE AND DATES COVERED
	February 1999	Technical Memorandum

4. TITLE AND SUBTITLE
Demonstration of Imaging Flow Diagnostics Using Rayleigh Scattering in Langley 0.3-Meter Transonic Cryogenic Tunnel

5. FUNDING NUMBERS
WU 522-31-61-01

6. AUTHOR(S)
B. Shirinzadeh, G. C. Herring, and Toya Barros

7. PERFORMING ORGANIZATION NAME(S) AND ADDRESS(ES)
NASA Langley Research Center
Hampton, VA 23681-2199

8. PERFORMING ORGANIZATION REPORT NUMBER
L-17801

9. SPONSORING/MONITORING AGENCY NAME(S) AND ADDRESS(ES)
National Aeronautics and Space Administration
Washington, DC 20546-0001

10. SPONSORING/MONITORING AGENCY REPORT NUMBER
NASA/TM-1999-208970

11. SUPPLEMENTARY NOTES
Shirinzadeh and Herring: Langley Research Center, Hampton, VA; Barros: Spelman College, Atlanta, GA.

12a. DISTRIBUTION/AVAILABILITY STATEMENT
Unclassified–Unlimited
Subject Category: 09, 34 Distribution: Standard
Availability: NASA CASI (301) 621-0390

12b. DISTRIBUTION CODE

13. ABSTRACT ***(Maximum 200 words)***

The feasibility of using the Rayleigh scattering technique for molecular density imaging of the free-stream flow field in the Langley 0.3-Meter Transonic Cryogenic Tunnel has been experimentally demonstrated. The Rayleigh scattering was viewed with a near-backward geometry with a frequency-doubled output from a diode-pumped CW Nd:YAG laser and an intensified charge-coupled device camera. Measurements performed in the range of free-stream densities from 3×10^{25} to 24×10^{25} molecules/m^3 indicate that the observed relative Rayleigh signal levels are approximately linear with flow field density. The absolute signal levels agree (within ≈30 percent) with the expected signal levels computed based on the well-known quantities of flow field density, Rayleigh scattering cross section for N_2, solid angle of collection, transmission of the optics, and the independently calibrated camera sensitivity. These results show that the flow field in this facility is primarily molecular (i.e., not contaminated by clusters) and that Rayleigh scattering is a viable technique for quantitative nonintrusive diagnostics in this facility.

14. SUBJECT TERMS	15. NUMBER OF PAGES
Rayleigh scattering; High Reynolds number facility; Cryotemperature	16
	16. PRICE CODE: A03

17. SECURITY CLASSIFICATION OF REPORT	18. SECURITY CLASSIFICATION OF THIS PAGE	19. SECURITY CLASSIFICATION OF ABSTRACT	20. LIMITATION OF ABSTRACT
Unclassified	Unclassified	Unclassified	UL